PERGAMON

International Journal of Solids and Structures 37 (2000) 4791–4810

INTERNATIONAL JOURNAL OF SOLIDS and STRUCTURES

www.elsevier.com/locate/ijsolstr

Design of microstructures of viscoelastic composites for optimal damping characteristics

Yeong-Moo Yi, Sang-Hoon Park, Sung-Kie Youn*

Department of Mechanical Engineering, Korea Advanced Institute of Science and Technology, 373-1, Gusung-dong, Yusung-ku, Taejon 305-701, Republic of Korea

Received 10 September 1998

Abstract

An inverse homogenization problem for two-phase viscoelastic composites is formulated as a topology optimization problem. The effective complex moduli are estimated by the numerical homogenization using the finite element method. Sensitivity analysis shows that the sensitivity calculations do not require the solution of any adjoint problem. The objective function is defined so that the topology optimization problem finds microstructures of viscoelastic composites which exhibit improved stiffness/damping characteristics within the specified operating frequency range. Design constraints include volume fraction, effective complex moduli, geometric symmetry and material symmetry. Several numerical design examples are presented with discussions on the nature of the designed microstructures. From the designed microstructures, it is found that mechanism-like structures and wavy structures are formed to maximize damping while retaining stiffness at the desired level.

Keywords: Viscoelastic composite; Optimal damping; Microstructure design; Inverse homogenization

1. Introduction

Increasing demands for the control of noise and vibration in structures have forced designers to take damping into account from the initial design stage. Viscoelastic composites have been widely applied for the purpose of reducing noise and vibration as well as for the purpose of increasing stiffness to weight ratio. These trends are mainly due to the fact that viscoelastic composites have desirable damping characteristics and provide design flexibility, i.e., tradeoff between damping and stiffness. Polymer composites, rubber-toughened composites, and engineering plastics are typical examples.

* Corresponding author. Fax: +82-42-861-1694.
E-mail address: skyoun@sorak.kaist.ac.kr (S.K. Youn).

PII: S0020-7683(99)00181-X

From the viewpoint of designers, it would be very useful if there is a material which possesses optimal properties under given environment. The property may be damping characteristics in the control of noise and vibration. However, it is practically impossible to invent an optimal material for each new design. Instead, it is more practical to construct and use a composite with materials at hand so that the composite exhibits good properties under given environment. It has been suggested that stiffness and damping characteristics of a viscoelastic composite may be improved by changing its microstructural topology (Yi et al., 1998).

The inverse homogenization approach (Sigmund, 1994) can be a good candidate in designing composites with specially tailored properties. In this approach, composites are assumed to have periodic microstructures. Following the structural topology optimization technique presented by Bendsøe and Kikuchi (1988), the microstructural configuration of a composite is represented by density distribution in the unit cell. Then, an optimal density distribution is sought so that the resulting composite exhibits the prescribed or optimal effective material properties. The (asymptotic) homogenization method is employed to calculate the effective material properties of the composite. This approach has been applied to the design of composites with extreme or unusual material properties: elastic composites with Poisson's ratio close to -1 and 0.5 (Sigmund, 1995) and thermoelastic composites with negative or zero thermal expansion coefficients (Sigmund and Torquato, 1997). It has also been applied to the design of piezoelectric sensors to improve the sensitivities of the output signals to the input signal (Nelli Silva et al., 1997).

In the present work, an inverse homogenization approach for two-phase viscoelastic composites is presented aiming at improving stiffness and damping characteristics. Several numerical examples and some discussions on the nature of the designed microstructures are presented.

2. Homogenization in viscoelasticity

2.1. Introduction

The (asymptotic) homogenization method, which originated from the study of partial differential equations with rapidly varying coefficients, applies to the estimation of the effective material properties of composites with periodic microstructures (Bensoussan et al., 1978; Sanchez-Palencia, 1980). The homogenization method assumes that field variable varies independently in the multiple length scales, i.e., in the local and in the global scales. Due to the periodicity of the microstructure, field variables such as displacement, strain, and stress are assumed to be periodic with respect to the local scale. In order to find the effective material properties of a medium, the asymptotic behavior of the medium as the period goes to zero is investigated. Mathematically, they are presented in the context of the asymptotic expansions. At this point, it should be noted that the homogenization method has a rigorous mathematical background; e.g., the solution of the original problem converges to the homogenized solution as the period goes to zero at least for linear elastic and viscoelastic problems — for proof, see Ref. (Sanchez-Palencia, 1980). Also, it is readily implemented with finite element method and thus especially useful for microstructures with complex and irregular configurations (Guedes and Kikuchi, 1990).

Although more insights can be obtained if we consider the homogenization of an viscoelastic medium in time domain (Yi et al., 1998), the homogenization in frequency domain (Nguyen et al., 1995) can be easily formulated by virtue of the Correspondence Principle. In this case, the homogenization process becomes identical to the one used in the elastic case except that the variables are complex. Since the present work deals with the microstructure design in which damping characteristics are of major concerns, the effective relaxation moduli in time domain are not needed and the homogenization will be done in frequency domain.

2.2. Basic concepts for homogenization

A brief summary of the homogenization problem for obtaining the effective complex moduli is presented following the same procedure as in the elastic case given by Sanchez-Palencia (1980). For more details, the readers are referred to: Bensoussan et al. (1978), Sanchez-Palencia (1980), Bakhvalov and Panasenko (1989), Oleinik et al. (1992) and Jikov et al. (1994) for theoretical aspects; Guedes and Kikuchi (1990) for finite element implementation; Nguyen et al. (1995) and Yi et al. (1998) for homogenization in viscoelasticity among the extensive references.

We designate the global coordinate by $\boldsymbol{x}$ and the local coordinate by $\boldsymbol{y}$. The global coordinate and the local coordinate are related with each other by a positive real parameter ε as follows:

$$\boldsymbol{y} = \frac{\boldsymbol{x}}{\varepsilon}. \tag{1}$$

In 2D, Y-periodicity of a function $f(\boldsymbol{y})$ in the local coordinate is defined as follows:

$$f(y_1 + n_1 Y_1, y_2 + n_2 Y_2) = f(y_1, y_2)$$

$$\forall \boldsymbol{y} = (y_1, y_2) \in \mathbb{R}^2 \quad \text{and} \quad \forall (n_1, n_2) \in \mathbb{N}^2 \tag{2}$$

where $\mathbb{N}$ is the set of integers, and Y_1 and Y_2 represent the period of the Y-periodicity, i.e.,

$$Y = (0,\ Y_1) \times (0,\ Y_2). \tag{3}$$

From an Y-periodic function $f(\boldsymbol{y})$ in the local coordinate, an εY-periodic function $f^{\varepsilon}(\boldsymbol{x})$ in the global coordinate can be defined as follows:

$$f^{\varepsilon}(\boldsymbol{x}) = f(\boldsymbol{x}/\varepsilon) = f(\boldsymbol{y}). \tag{4}$$

Derivatives in the global scale and in the local scale can be related by using Eq. (1). Suppose that a function $g^{\varepsilon}(\boldsymbol{x}) = g(\boldsymbol{x}, \boldsymbol{y})$ depends on both the global and the local coordinates. Then, the following relation holds:

$$\frac{\partial g^{\varepsilon}(\boldsymbol{x})}{\partial x_i} = \frac{\partial g(\boldsymbol{x}, \boldsymbol{y})}{\partial x_i} + \frac{1}{\varepsilon}\frac{\partial g(\boldsymbol{x}, \boldsymbol{y})}{\partial y_i}; \quad \boldsymbol{y} = \frac{\boldsymbol{x}}{\varepsilon}. \tag{5}$$

For the averaging process of the homogenization, the following mean operator, $\tilde{\bullet}$, on Y is defined.

$$\tilde{\bullet} = \frac{1}{|Y|}\int_Y \bullet \,\mathrm{d}Y \tag{6}$$

where $|Y|$ is the measure of Y.

2.3. Linear viscoelasticity in frequency domain

A problem of 2D linear viscoelasticity with a periodic microstructure as shown in Fig. 1 is considered, where the inertia effects and the body forces are not present. It is assumed that the problem is under plane stress state and steady-state sinusoidal oscillation. Using the Correspondence Principle

(Christensen, 1982), the problem at a fixed frequency ω is as follows:

$$\frac{\partial \bar{\sigma}_{ij}^{\varepsilon}(\boldsymbol{x})}{\partial x_j} = 0 \text{ in } \Omega \tag{7a}$$

$$\bar{\sigma}_{ij}^{\varepsilon}(\boldsymbol{x}) = G_{ijkl}^{\varepsilon}(\boldsymbol{x}, \omega)\bar{e}_{kl}\big(\bar{\boldsymbol{u}}^{\varepsilon}(\boldsymbol{x})\big) \tag{7b}$$

$$\bar{e}_{kl}\big(\bar{\boldsymbol{u}}^{\varepsilon}(\boldsymbol{x})\big) = \frac{1}{2}\left(\frac{\partial \bar{u}_k^{\varepsilon}(\boldsymbol{x})}{\partial x_l} + \frac{\partial \bar{u}_l^{\varepsilon}(\boldsymbol{x})}{\partial x_k}\right) \tag{7c}$$

where Ω is an open connected domain of $\mathbb{R}^2$. In the above equations, $\bar{\boldsymbol{u}}^{\varepsilon}$, $\bar{e}_{kl}$, and $\bar{\sigma}_{kl}^{\varepsilon}$ are the spatial part of the displacement, strain, and stress, respectively:

$$\boldsymbol{u}^{\varepsilon}(\boldsymbol{x}, t) = \bar{\boldsymbol{u}}^{\varepsilon}(\boldsymbol{x}) \exp(i\omega t) \tag{8a}$$

$$e_{kl}^{\varepsilon}(\boldsymbol{x}, t) = \bar{e}_{kl}^{\varepsilon}(\boldsymbol{x}) \exp(i\omega t) \tag{8b}$$

$$\sigma_{kl}^{\varepsilon}(\boldsymbol{x}, t) = \bar{\sigma}_{kl}^{\varepsilon}(\boldsymbol{x}) \exp(i\omega t). \tag{8c}$$

The complex modulus tensor $G_{ijkl}^{\varepsilon}(\boldsymbol{x}, \omega)$ is given by

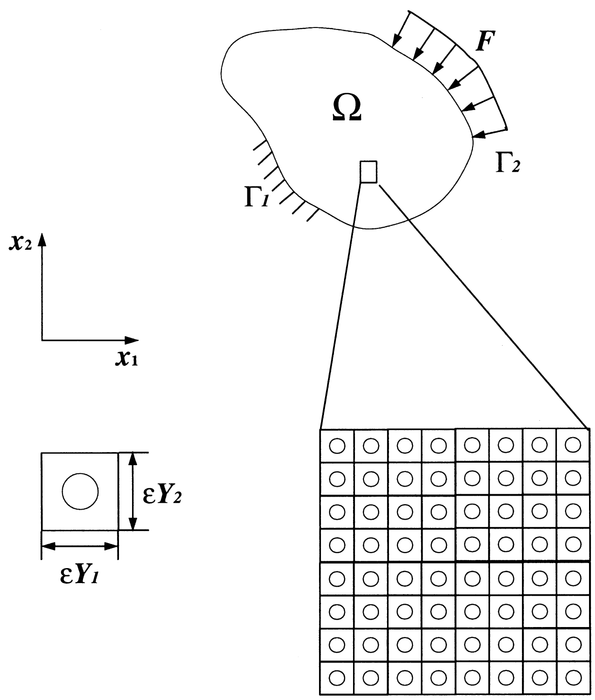

Fig. 1. A problem with periodic microstructure.

$$G^{\varepsilon}_{ijkl}(\boldsymbol{x},\omega) = G_{ijkl}\left(\frac{\boldsymbol{x}}{\varepsilon},\omega\right) = G_{ijkl}(\boldsymbol{y},\omega) \tag{9}$$

where $G_{ijkl}(\boldsymbol{y},\omega)$ is Y-periodic in the local coordinate $\boldsymbol{y}$.

Note that the problem defined above is identical to the elasticity problem except that the variables in the present problem are complex. The asymptotic behavior is to be observed as ε approaches to zero.

2.4. Asymptotic expansions

The most important and essential postulate in the homogenization method is that $\bar{u}^{\varepsilon}_i(\boldsymbol{x})$ has an asymptotic expansion in the following form.

$$\bar{u}^{\varepsilon}_i(\boldsymbol{x}) = \bar{u}^0_i(\boldsymbol{x}) + \varepsilon\bar{u}^1_i(\boldsymbol{x},\boldsymbol{y}) + \varepsilon^2\bar{u}^2_i(\boldsymbol{x},\boldsymbol{y}) + \cdots; \quad \boldsymbol{y} = \frac{\boldsymbol{x}}{\varepsilon} \tag{10}$$

where $\bar{u}^m_i(\boldsymbol{x},\boldsymbol{y})$ is Y-periodic in $\boldsymbol{y}$ and independent of ε. From Eqs. (5) and (10), the asymptotic expansions for $\bar{e}^{\varepsilon}_{ij}(\boldsymbol{x})$ and $\bar{\sigma}^{\varepsilon}_{ij}(\boldsymbol{x})$ are obtained as follows:

$$\bar{e}^{\varepsilon}_{ij}(\boldsymbol{x}) = \bar{e}_{ij}\big(\bar{\boldsymbol{u}}^{\varepsilon}(\boldsymbol{x},\boldsymbol{y})\big) = \bar{e}^0_{ij}(\boldsymbol{x}) + \varepsilon\bar{e}^1_{ij}(\boldsymbol{x},\boldsymbol{y}) + \cdots; \quad \boldsymbol{y} = \frac{\boldsymbol{x}}{\varepsilon} \tag{11a}$$

$$\bar{\sigma}^{\varepsilon}_{ij}(\boldsymbol{x}) = G^{\varepsilon}_{ijkl}\bar{e}_{kl}\big(\bar{\boldsymbol{u}}^{\varepsilon}(\boldsymbol{x})\big) = \bar{\sigma}^0_{ij}(\boldsymbol{x},\boldsymbol{y}) + \varepsilon\bar{\sigma}^1_{ij}(\boldsymbol{x},\boldsymbol{y}) + \cdots; \quad \boldsymbol{y} = \frac{\boldsymbol{x}}{\varepsilon} \tag{11b}$$

where

$$\bar{e}^0_{ij}(\boldsymbol{x},\boldsymbol{y}) = \bar{e}_{ijx}(\bar{\boldsymbol{u}}^0) + \bar{e}_{ijy}(\bar{\boldsymbol{u}}^1) \tag{12a}$$

$$\bar{\sigma}^0_{ij}(\boldsymbol{x},\boldsymbol{y}) = G^{\varepsilon}_{ijkl}(\boldsymbol{x},\omega)\bar{e}_{kl}\big(\bar{\boldsymbol{u}}^0(\boldsymbol{x})\big) = G_{ijkl}(\boldsymbol{y},\omega)\bar{e}_{kl}\big(\bar{\boldsymbol{u}}^0(\boldsymbol{x})\big). \tag{12b}$$

In Eq. (12a), the subscripts x and y imply the differentiation with respect to x_i and y_i, respectively:

$$\bar{e}_{ijx}(\bar{\boldsymbol{v}}) = \frac{1}{2}\left(\frac{\partial\bar{v}_i}{\partial x_j} + \frac{\partial\bar{v}_j}{\partial x_i}\right) \quad \text{and} \quad \bar{e}_{ijy}(\bar{\boldsymbol{v}}) = \frac{1}{2}\left(\frac{\partial\bar{v}_i}{\partial y_j} + \frac{\partial\bar{v}_j}{\partial y_i}\right). \tag{13}$$

2.5. Local problem, global problem, and homogenized complex moduli

By introducing Eqs. (5) and (11b) into Eq. (7a), and arranging it against ε^{-1} and ε^0, we obtain the following two equations.

$$\frac{\partial\bar{\sigma}^0_{ij}(\boldsymbol{x},\boldsymbol{y})}{\partial y_j} = 0 \tag{14a}$$

$$\frac{\partial\bar{\sigma}^1_{ij}(\boldsymbol{x},\boldsymbol{y})}{\partial y_j} + \frac{\partial\bar{\sigma}^0_{ij}(\boldsymbol{x},\boldsymbol{y})}{\partial x_j} = 0. \tag{14b}$$

By applying the mean operator and imposing the periodicity condition, Eq. (14b) becomes

$$\frac{\partial \tilde{\bar{\sigma}}_{ij}^{0}(\boldsymbol{x})}{\partial x_j} = 0. \tag{15}$$

Eqs. (14a) and (15) represent the local and the global problems, respectively. By solving the local problem (14a), we can obtain the homogenized complex moduli. Since the present work is not for the illustration of the homogenization method and somewhat lengthy manipulations are needed to arrive at the final equations, we do not describe the procedure in detail. Following the same procedure as in Ref. (Sanchez-Palencia, 1980) the local problem in frequency domain becomes as follows:

Find $\boldsymbol{\chi}^{kl} \in V_Y$ such that

$$\int_Y G_{ijpq}(\boldsymbol{y}, \omega) \frac{\partial \chi_p^{kl}}{\partial y_q} \frac{\partial v_i}{\partial y_j} \, \mathrm{d}Y = \int_Y G_{ijkl}(\boldsymbol{y}, \omega) \frac{\partial v_i}{\partial y_j} \, \mathrm{d}Y, \quad \forall \boldsymbol{v} \in V_Y \tag{16}$$

where

$$V_Y = \left\{ \boldsymbol{u} | u_i \in H_{\mathrm{loc}}^1(\mathbb{R}^2), \ Y\text{-periodic} \right\}. \tag{17}$$

And the homogenized stress–strain relations in frequency domain are given as follows:

$$\tilde{\bar{\sigma}}_{ij}^{0}(\boldsymbol{x}) = G_{ijkl}^{h}(\omega) \bar{e}_{kl}\left(\bar{\boldsymbol{u}}^{0}(\boldsymbol{x})\right) \tag{18}$$

with the following homogenized or effective complex moduli.

$$G_{ijkl}^{h}(\omega) = \frac{1}{|Y|} \int_Y G_{pqrs}(\boldsymbol{y}, \omega) \left(\delta_{kp}\delta_{lq} - \frac{\partial \chi_p^{kl}}{\partial y_q} \right) \left(\delta_{ir}\delta_{js} - \frac{\partial \chi_r^{ij}}{\partial y_s} \right) \mathrm{d}Y \tag{19}$$

where χ_p^{kl} is the solution of the local problem (16). By solving the local problem (16) and using Eq. (19) the effective complex moduli at a given frequency are obtained.

It is noted that Eqs. (15), (18), and (13) constitute the homogenized problem, which has the same form as the original problem (7a)–(7c) except that, in the homogenized problem, the material properties no longer depend on the local coordinate $\boldsymbol{y}$. It is also noted that the functions in Eqs. (16) and (19) are complex. Thus, for the numerical solutions of the effective complex moduli, we need a finite element implementation with complex variables.

3. Inverse homogenization problem

3.1. Introduction

From the study of the homogenization of general viscoelastic composites in time and frequency domain (Yi et al., 1998), it has been suggested that damping characteristics may be improved by modifying the microstructural configurations of viscoelastic composites. The inverse homogenization (Sigmund, 1994), which is based on the homogenization method and the structural topology optimization, seems to be a natural approach for this purpose.

In structural topology optimization (Bendsøe and Kikuchi, 1988), a generalized shape optimization problem is considered by introducing material density at each point of the design domain. Then, the topology optimization problem becomes an optimization problem to find an optimal density distribution in the design domain. Mathematically, this corresponds to the relaxation of a variational problem (Kohn and Strang, 1986). The homogenization method has been naturally applied to extract a relation between the material property and the material density by employing composite models such as the rectangular cell with a rectangular hole (Bendsøe and Kikuchi, 1988) or rank-2 layering (Bendsøe, 1989). However, artificial material models can also be employed to obtain a simple moduli–density relationship (Bendsøe et al., 1993; Yang and Chuang, 1994; Youn and Park, 1997). For more details on the structural topology optimization, the readers are referred to Bendsøe et al. (1994), Bendsøe (1995), Rozvany et al. (1995) and Allaire et al. (1997).

In this section, an inverse homogenization problem of two-phase viscoelastic composites is formulated as a topology optimization problem following a similar approach as that of Sigmund and Torquato (1997).

3.2. Design variables and artificial two-phase material model

An inverse homogenization problem is defined as a topology optimization in which a distribution of two viscoelastic phases in a unit cell is to be found so as to optimize the stiffness and damping characteristics of the resulting viscoelastic composite. In order to set up a topology optimization problem, at each point in the design domain, we need complex moduli as a function of the material density. In a practical viewpoint, the relationship needs not to be based on a concrete model. This explains wide use of the so-called artificial material model, which significantly simplifies the topology optimization problem. Note that, however, the homogenization is involved in the evaluation of the objective function and the constraints.

We employ an artificial two-phase material model, which is similar to that proposed by Sigmund and Torquato (1997). At each point $\boldsymbol{y}$ in the design domain, i.e. the unit cell, the complex moduli are defined as follows:

$$G_{ijkl}(\boldsymbol{y}, \omega) = \rho(\boldsymbol{y}) G_{ijkl}^{(1)}(\omega) + \big(1 - \rho(\boldsymbol{y})\big) G_{ijkl}^{(2)}(\omega) \tag{20}$$

where $G_{ijkl}^{(1)}$ and $G_{ijkl}^{(2)}$ are the complex moduli of phase 1 and phase 2 materials, respectively, and ρ the density of phase 1 material at the point $\boldsymbol{y}$. Of course, the density of phase 2 material is $1 - \rho$.

Design domain, which is a periodic unit cell, is discretized with N finite elements. The density is assumed to be constant in each element but it can be varied from one element to another. The density in each element becomes the design variable of the optimization problem. With the present artificial material model, the topology optimization problem becomes similar to the thickness optimization problem with two layers in which the total thickness is constant through the design domain.

3.3. Sensitivity analysis

Sensitivities are required for the efficient computation of the iterative design modifications in the optimization process. Since, as will be seen later, the objective function and the constraints are defined as functions of the storage modulus, the loss modulus, and the loss tangent of the homogenized medium, the sensitivities of the effective complex moduli with respect to density change are necessary. By differentiating Eq. (19) with respect to the density of the eth element, we have:

$$\frac{\partial G^{h}_{ijkl}(\omega)}{\partial \rho_e} = \frac{1}{|Y|}\int_Y \frac{\partial G_{pqrs}(\boldsymbol{y},\omega)}{\partial \rho_e}\left(\delta_{kp}\delta_{lq} - \frac{\partial \chi_p^{kl}}{\partial y_q}\right)\left(\delta_{ir}\delta_{js} - \frac{\partial \chi_r^{ij}}{\partial y_s}\right)\mathrm{d}Y - \frac{1}{|Y|}\int_Y G_{pqrs}(\boldsymbol{y},\omega)\frac{\partial^2 \chi_p^{kl}}{\partial \rho_e \partial y_q}\left(\delta_{ir}\delta_{js} - \frac{\partial \chi_r^{ij}}{\partial y_s}\right)\mathrm{d}Y - \frac{1}{|Y|}\int_Y G_{pqrs}(\boldsymbol{y},\omega)\left(\delta_{kp}\delta_{lq} - \frac{\partial \chi_p^{kl}}{\partial y_q}\right)\frac{\partial^2 \chi_r^{ij}}{\partial \rho_e\,\partial y_s}\,\mathrm{d}Y \tag{21}$$

where ρ_e is the density in the eth element. Let us consider the second term of the right-hand side in the above equation. It can be rewritten as follows:

$$-\frac{1}{|Y|}\int_Y G_{pqrs}(\boldsymbol{y},\omega)\frac{\partial^2 \chi_p^{kl}}{\partial \rho_e\,\partial y_q}\left(\delta_{ir}\delta_{js} - \frac{\partial \chi_r^{ij}}{\partial y_s}\right)\mathrm{d}Y = \frac{1}{|Y|}\int_Y G_{pqrs}(\boldsymbol{y},\omega)\frac{\partial \chi_r^{ij}}{\partial y_s}\frac{\partial}{\partial y_q}\left(\frac{\partial \chi_p^{kl}}{\partial \rho_e}\right)\mathrm{d}Y - \frac{1}{|Y|}\int_Y G_{pqij}(\boldsymbol{y},\omega)\frac{\partial}{\partial y_q}\left(\frac{\partial \chi_p^{kl}}{\partial \rho_e}\right)\mathrm{d}Y. \tag{22}$$

Note that $\partial \boldsymbol{\chi}^{kl}/\partial \rho_e$ is in V_Y since the solutions of Eq. (16) are in V_Y for any density distribution and their linear combinations are also in V_Y. Therefore, noting that $\boldsymbol{\chi}^{kl}$ satisfies Eq. (16) for any function in V_Y, the second term of Eq. (21) becomes zero by applying Eq. (16) to Eq. (22). Similarly, the third term of Eq. (21) also becomes zero. Thus, Eq. (21) is reduced as follows:

$$\frac{\partial G^{h}_{ijkl}(\omega)}{\partial \rho_e} = \frac{1}{|Y|}\int_Y \frac{\partial G_{pqrs}(\boldsymbol{y},\omega)}{\partial \rho_e}\left(\delta_{kp}\delta_{lq} - \frac{\partial \chi_p^{kl}}{\partial y_q}\right)\left(\delta_{ir}\delta_{js} - \frac{\partial \chi_r^{ij}}{\partial y_s}\right)\mathrm{d}Y. \tag{23}$$

Also, from Eq. (20) the following simple relation holds for the suggested artificial two-phase material model.

$$\frac{\partial G_{ijkl}(\boldsymbol{y},\omega)}{\partial \rho_e} = \begin{cases} G^{(1)}_{ijkl}(\omega) - G^{(2)}_{ijkl}(\omega) & \text{if } \boldsymbol{y} \in Y_e \\ 0 \quad \text{otherwise} \end{cases} \tag{24}$$

where Y_e is the domain of the eth element. From Eqs. (23) and (24) we finally arrive at the following simple formula for the sensitivities of the effective complex moduli with respect to the element density.

$$\frac{\partial G^{h}_{ijkl}(\omega)}{\partial \rho_e} = \frac{1}{|Y|}\int_{Y_e}\left(G^{(1)}_{ijkl}(\omega) - G^{(2)}_{ijkl}(\omega)\right)\left(\delta_{kp}\delta_{lq} - \frac{\partial \chi_p^{kl}}{\partial y_q}\right)\left(\delta_{ir}\delta_{js} - \frac{\partial \chi_r^{ij}}{\partial y_s}\right)\mathrm{d}Y_e. \tag{25}$$

Note that it is not required to solve any adjoint problem to obtain the sensitivities. This is not the case for more complex problems such as the homogenization of piezoelectric composites (Nelli Silva et al., 1997).

3.4. Objective function

The objective of the present work is to find a microstructure so that the designed viscoelastic composite exhibits desirable stiffness and damping characteristics under given operating environments. In general, design requirements on stiffness and damping characteristics are problem dependent. In a case, a desirable design may be one that maximizes damping at a frequency range while maximizes stiffness at another frequency range. In another case, a design that exhibits high stiffness, regardless of damping, along one direction while exhibits high damping, regardless of stiffness, along another direction may be desired. Also, in some cases, damping to stiffness ratio may be of concern rather than the damping itself. In order to cover up these various kinds of objectives in diverse situations, the objective function in the present study is defined as a combination of storage modulus, loss modulus, and loss tangent at operating frequencies with linear and exponential weighting factors on each component.

$$
\begin{aligned}
f_1 = {} & \sum_{i=1}^{3}\sum_{j=i}^{3}\sum_{m=1}^{M}\zeta_{\text{storage}}(i,j,m)\big(G'_{ij}(\omega_m)\big)^{\eta_{\text{storage}}(i,j,m)} \\
& + \sum_{i=1}^{3}\sum_{j=i}^{3}\sum_{m=1}^{M}\zeta_{\text{loss}}(i,j,m)\big(G''_{ij}(\omega_m)\big)^{\eta_{\text{loss}}(i,j,m)} + \sum_{i=1}^{3}\sum_{j=i}^{3}\sum_{m=1}^{M}\zeta_{\tan}(i,j,m)\big(\tan\delta_{ij}(\omega_m)\big)^{\eta_{\tan}(i,j,m)}
\end{aligned}
\tag{26}
$$

where M is the number of operating frequencies, ω_m is the mth operating frequency, $G'_{ij}(\omega_m)$ is the ij-component of storage modulus at ω_m, $G''_{ij}(\omega_m)$ is the ij-component of loss modulus at ω_m, $\tan\delta_{ij}(\omega_m)$ is the ij-component of loss tangent at ω_m, ζ is the linear weighting factors, and η is the exponential weighting factors.

Note that this form of combining individual objectives is common in multi-objective optimization. The linear weighting factors are used mainly for quantifying the relative contribution from each objective. The exponential weighting factors are used to account for the situations where different designs, which have the same linear sum of the individual objectives result, in different performances. Exponential weighting factors greater than one tend to penalize the individual objectives and those smaller than one tend to make a compromise between the competing objectives. In many cases, the exponential weighting factors can significantly affect the convergence characteristics of the optimization process. Also, there are numerous local minima in the inverse homogenization problems (Sigmund and Torquato, 1997). These two facts lead to the conclusion that, when selecting the weighting factors, the effects of weighting factors on the convergence characteristics should also be taken into account. However, at present, there is no particular rule for the selection of the weighting factors except that too large exponential weighting factors are prohibited. In practice, the weighting factors can be easily manipulated to obtain useful microstructures.

For clearer interpretation of the result, it is desirable to suppress intermediate values in the optimized density distribution. This can be accomplished by including a penalty term in the objective function (Allaire and Kohn, 1993). Following the approach, the objective function used in the present work is follows:

$$
f_2 = f_1 + \zeta_{\text{penalty}}\left[\sum_{e=1}^{N}\rho_e(1-\rho_e)\right]^{\eta_{\text{penalty}}}
\tag{27}
$$

where f_1 is as defined in Eq. (26) and ζ_{penalty} and η_{penalty} are weighting factors for the penalty term on the intermediate densities.

3.5. Design constraints

In the present formulation, the design variables are the densities of phase 1 material in the elements. Since these design variables are effective only on [0, 1], side constraints are imposed on them.

$$0 \le \rho_e \le 1 \quad \forall e = 1, \ldots, N. \tag{28}$$

Volume fraction of each phase can also be constrained as follows:

$$V_{\min} \le \sum_{e}^{N} \rho_e V_e \le V_{\max} \tag{29}$$

where V_e is the volume (area in 2D) of the eth element and $V_{\min}$ and $V_{\max}$ the lower and the upper bounds for the volume of phase 1 material, respectively. The lower and the upper bounds for phase 2 material are $|Y| - V_{\max}$ and $|Y| - V_{\min}$, respectively, since we assume that the density of phase 2 material is $1 - \rho_e$.

Symmetry conditions can be applied to the geometry of a microstructure by design variable linking, i.e., assigning the same density value to the elements in symmetric position (Sigmund and Torquato, 1997). In the present work, the geometric symmetry can be imposed about the X_1-axis or about the X_2-axis as well as about both the X_1- and X_2-axes. The geometric symmetry not only reduces the number of design variables but also ensures the orthotropy of a composite. Another benefit is that the interpretations of the results can be easier. In some cases, the small number of design variables due to the geometric symmetry can improve the convergence by attenuating the problem of numerous local minima.

Constraints on the effective complex moduli or on some functions of the moduli may be useful. At this point, it is noted that material symmetries such as square symmetry and isotropy can be represented using a linear combination of components of the moduli. Assuming orthotropy, which can be easily imposed by the geometric symmetry, we have the following conditions on material symmetries for 2D plane stress state (Sigmund and Torquato, 1997).

- Square symmetry condition: $G_{11} = G_{22}$
- Isotropy condition: $G_{11} = G_{22}$ and $G_{11} = G_{12} + 2G_{33}$.

All these kinds of constraints, including side constraints on some components of the effective complex moduli and the material symmetries, can be treated in a general form as follows:

$$L^{(k)} \le c_1^{(k)} g_1^{(k)} + c_2^{(k)} g_2^{(k)} + c_3^{(k)} g_3^{(k)} \le U^{(k)} \tag{30}$$

where g is one of storage modulus, loss modulus, or loss tangent at some frequency, c the coefficients, and k the constraint number.

3.6. Problem statements and optimization scheme

With the design variable, the objective function, and the design constraints defined previously, an inverse homogenization problem for optimal microstructure design can be stated as a topology optimization problem as follows:

$$
\begin{aligned}
&\text{maximize} && f_2(\rho_1, \ldots, \rho_N) \\
&\text{subject to} && 0 \le \rho_e \le 1 \\
& && V_{\min} \le \sum_{e}^{N} \rho_e V_e \le V_{\max} \\
& && L^{(k)} \le a_1^{(k)} g_1^{(k)} + a_2^{(k)} g_2^{(k)} + a_3^{(k)} g_3^{(k)} \le U^{(k)} \\
& && \text{geometric symmetry}
\end{aligned}
\tag{31}
$$

where f_2 is defined in Eq. (27).

For the optimization algorithm, the sequential linear programming (SLP) is used. In SLP, the optimization problem is linearized around the current design point in each iteration and the next design is found by the linear programming. In this work, the method of feasible directions is used as the constrained linear programming method. The reason for using SLP is its robustness since the inverse homogenization problem has numerous local minima and is not a well-behaved problem (Sigmund and Torquato, 1997). For the implementation of the optimization algorithm, DOT (Design Optimization Tool) version 4.00, which is a general purpose FORTRAN subroutines for optimization, is used (VMA Engineering, 1993). It is noted that, although the homogenization problem (16) deals with complex variables, the objective function and constraints are all real variables since they are based on the storage modulus and the loss modulus. For more details on the optimization scheme used in the present work

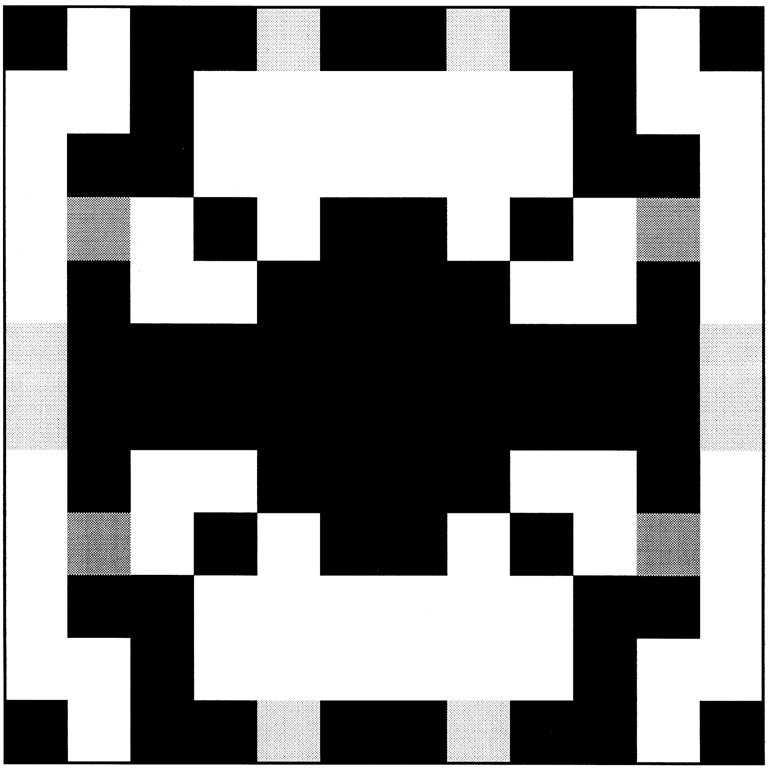

Fig. 2. Microstructure for example 1.

Table 1
Effective complex moduli of example 1

	Frequency, ω	Storage modulus, $G'_{11}(\omega)$	Loss modulus, $G''_{11}(\omega)$	Loss tangent, $\tan\delta_{11}(\omega)$
Material 1	0.5	73.56	0.00	0.000
Material 2	0.5	1.71	1.14	0.667
Composite 1	0.5	4.58	2.83	0.618
Composite 2	0.5	24.84	1.10	0.044
Optimal composite	0.5	15.01	2.76	0.184

(SLP with the method of feasible directions), readers can refer to Arora (1989) for the theoretical aspects and VMA Engineering (1993) for the implementational details.

4. Numerical examples and discussions

4.1. Introduction

In this section, numerical examples for the microstructure design to improve stiffness and damping characteristics of viscoelastic composites are presented. The design domain is discretized with 12×12 square bilinear finite elements in a unit cell. The design optimization starts with an initial density distribution of the two-phase material. The initial density in each element is randomly generated with minimal conditions: the side constraints (28) and the volume constraint (29). Initial density distribution should not be uniform. For the uniform density distribution, design change cannot occur since the sensitivities in all elements are identical.

Because of numerous local minima, the resulting density distribution strongly depends on the initial guess and the parameters used in the specific optimization scheme as well as the weighting factors. As a result, it may not be only meaningless but also confusing the readers to present the specific values of the weighting factors, the initial guesses, and the parameters used in the examples since it is practically impossible to reproduce the same results. Therefore, in the following examples, only the essential features of objective function and constraints will be presented. However, it is found in the numerical examples that although the density distributions are varied significantly according to the choices of weighting factors and initial guesses, the objective function values do not differ largely provided that weighting factors and initial guesses are properly chosen so as to converge to a solution smoothly.

In the figures of the unit cells, as shown in Fig. 2, black elements represent material 1, white elements represent material 2, and gray elements represent intermediate phase.

4.2. Example 1

As a first example, microstructure design of a viscoelastic composite composed of an elastic phase and a viscoelastic phase is considered. Although the material properties are non-dimensional, their relative magnitudes are taken from the approximate material properties of typical glass for the elastic material and typical epoxy for the viscoelastic material. The viscoelastic material is modeled by the standard linear solid (Christensen, 1982) and the relaxation time is artificially assumed. The material properties are as follows.

$$\begin{array}{lll} E = 70, & \nu = 0.22 & \text{for phase 1 material} \\ E(t) = 1 + 2.5e^{-t}, & \nu = 0.35 & \text{for phase 2 material.} \end{array}$$

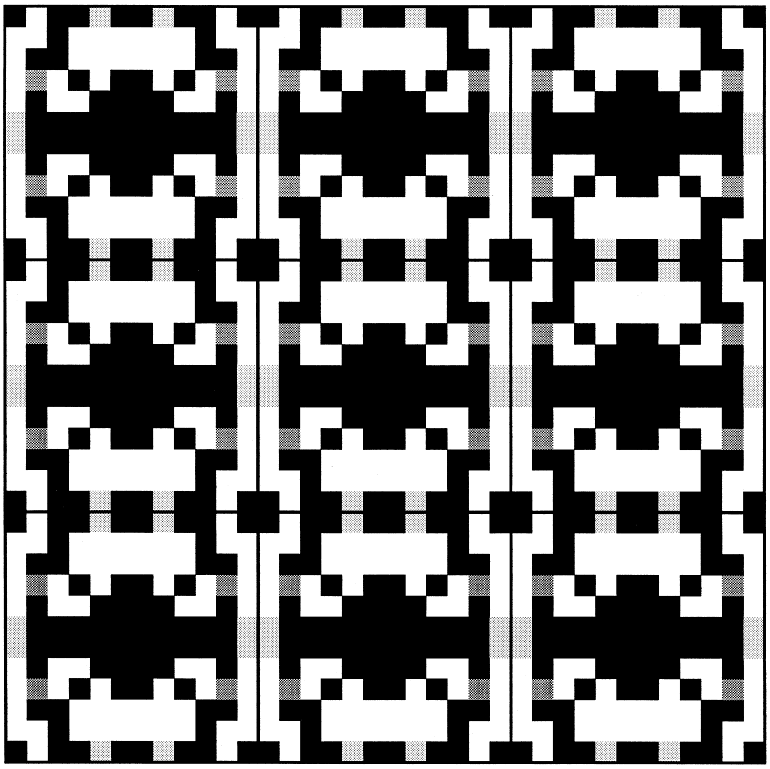

Fig. 3. Periodic microstructure for example 1.

Suppose we are to design a microstructure of a viscoelastic composite which is composed of the above two materials with 50% volume fraction for each material. The composite is to be used in vibrating structures and the operating frequency is artificially assumed to be 0.5.

A simple way for constructing microstructures is to use a square unit cell with a circular inclusion. Let us define two kinds of composites with this microstructural configuration for later references. For the composite 1, the elastic material is used for the circular inclusion and the viscoelastic material for the matrix. For the composite 2, the roles of the two materials are interchanged. Table 1 shows the effective complex moduli of these two composites at the operating frequency. In many engineering applications, certain degrees of lower bounds are required for both stiffness and damping. For example, to reduce vibration effectively by using a damper, stiffness of a damper should not be too low. Suppose that we need a composite whose stiffness, $G'_{11} = G'_{22}$, should be greater than 15 and the corresponding loss tangent should be as large as possible at the given frequency. With a simple microstructural configuration such as the composite 1 and the composite 2 defined above, we cannot obtain a satisfactory design. Even if we increase the volume fraction of the elastic inclusion in the composite 1 up to 70%, $G'_{11} = G'_{22}$ have a value of only 10.16. In that case, the diameter of the circular inclusion becomes 0.944 if the unit cell size is 1. If we use the composite 2 to obtain sufficient stiffness, then damping characteristics becomes worse.

The first design example has been selected with the above observations in mind. The objective of this example is to find a microstructure which yields as large damping as possible while the minimally required stiffness is to be achieved at the operating frequency, $\omega = 0.5$. The description of the objective

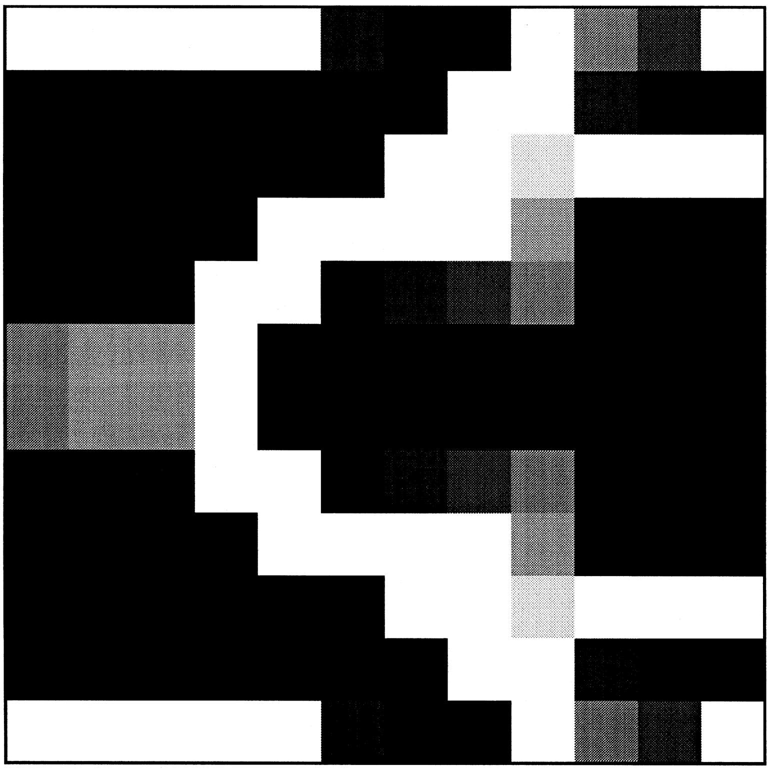

Fig. 4. Microstructure for Example 2.

function and the constraints are as follows.

$$\begin{array}{ll} \text{maximize} & \tan\delta_{11}(\omega)\big(=\tan\delta_{22}(\omega)\big), \quad \text{where } \omega = 0.5 \\ \text{subject to} & G'_{11}(\omega) = G'_{22}(\omega) \geq 15.0 \\ & 50\% \text{ volume fraction for each material} \\ & \text{geometric symmetry about } X_1\text{-axis and } X_2\text{-axis.} \end{array}$$

Also, the penalty term has been added as in Eq. (27) to reduce the regions of intermediate density. Fig. 2 shows the unit cell with the optimal microstructure, for which the solution converged after 148 function calls. Fig. 3 also shows the same microstructure in a 3×3 cells for easier understanding of the designed microstructure. The effective complex moduli are listed in Table 1. It can be concluded that the newly designed microstructure shows successful tradeoff between stiffness and damping. Some interpretations are possible for the designed microstructure. The elastic phase is nearly connected so as to provide sufficient stiffness. At the same time, the elastic phase forms a mechanism-like structure in some region with lumps of viscoelastic phase around the linkage. This mechanism-like structure in the elastic phase result in sufficient deformation in the viscoelastic phase. These two facts explain the tradeoff between stiffness and damping. The mechanism-like structures are also found in the microstructures with extreme properties such as negative Poisson's ratio and it has been pointed out that the mechanism-like structures have a crucial role in such extreme microstructures (Sigmund, 1995). Although the designed microstructures are different with different initial guesses and weighting factors used, the essential

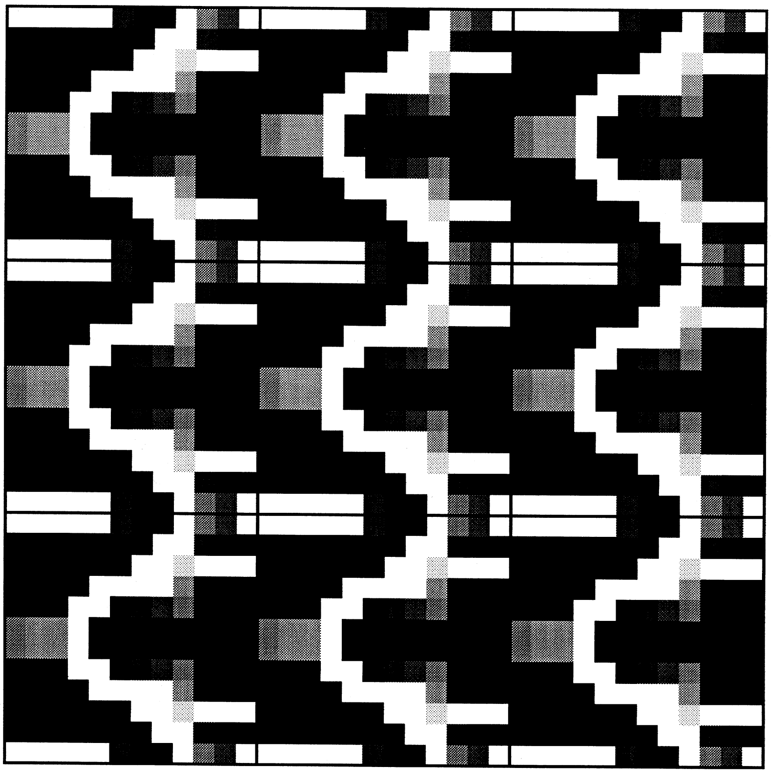

Fig. 5. Periodic microstructure for Example 2.

features of the optimal microstructures are the same. The main differences are in their convergence speed and interpretability (by human).

4.3. Example 2

Suppose that the constituent materials and the operating frequency are same as in Example 1. However, in this time, suppose that the structure experiences higher vibration level in one direction. For example, the payloads mount structure for installing electronic devices in a launch vehicle experiences higher vibration level in longitudinal direction than in lateral direction. Suppose that we want to design a viscoelastic composite, which should exhibits a good damping characteristics in that direction in order to use the composite as an anti-vibration damper. To reduce vibration effectively by using a damper, stiffness of a damper should not be too low. Suppose that we need a composite whose stiffness, $G'_{11} = G'_{22}$, should be greater than 15, and the corresponding loss tangent should be as large as possible at a given frequency in a specified direction. With such a simple microstructural configuration as the composite 1 and the composite 2 in Example 1, we cannot obtain the satisfactory design as stated in Example 1.

The second design example has been selected with the above observations in mind. The objective of this example is to find a microstructure that yields as large damping as possible in a specified direction while the desired stiffness of the microstructure is maintained. The description of the objective function and the constraints are as follows.

Table 2
Effective complex moduli of example 2

	Frequency, ω	Storage modulus, $G'_{11}(\omega)$	Loss modulus, $G''_{11}(\omega)$	Loss tangent, $\tan\delta_{11}(\omega)$
Material 1	0.5	73.56	0.00	0.000
Material 2	0.5	1.71	1.14	0.667
Composite 1	0.5	4.58	2.83	0.618
Composite 2	0.5	24.84	1.10	0.044
Optimal composite	0.5	15.02	6.58	0.438

$$\begin{aligned} &\text{maximize} && \tan\delta_{11}(\omega), \quad \text{where } \omega = 0.5 \\ &\text{subject to} && G'_{11}(\omega) = G'_{22}(\omega) \geq 15.0 \\ & && \text{geometric symmetry about } X_1\text{-axis.} \end{aligned}$$

Note that in the present example the loss tangent can be different along different directions and the volume constraint is not given. Fig. 4 shows the unit cell of an optimal microstructure. Fig. 5 also shows the same microstructures in a 3×3 cells for easier understanding of the designed microstructure. The effective complex moduli are listed in Table 2. Some interpretations are possible for the designed microstructure as in Example 1. The elastic phase are nearly connected together so as to provide sufficient stiffness as in Example 1. At the same time, the viscoelastic phase forms a wavy pattern between elastic phase, which also forms a wavy pattern. This microstructure with wavy viscoelastic phase and elastic phase result in sufficient deformations in the viscoelastic phase in the specified direction. These facts explains the tradeoff between stiffness and damping in the composites.

4.4. Example 3

As the final example, microstructure design of a viscoelastic composite composed of two different viscoelastic materials is considered. The relative magnitudes of the material properties are taken from the approximate material properties of polyimide materials. The viscoelastic material behavior is again modeled by the standard linear solid and the relaxation times are artificially assumed. The material properties are as follows.

Table 3
Effective complex moduli of example 3

	Frequency, ω	Storage modulus, $G'_{11}(\omega)$	Loss modulus, $G''_{11}(\omega)$	Loss tangent, $\tan\delta_{11}(\omega)$
Material 1	0.04	1.04	1.18	1.132
	0.4	3.79	0.80	0.212
Material 2	0.04	0.58	0.14	0.237
	0.4	1.04	1.18	1.132
Composite 1	0.04	0.84	0.43	0.510
	0.4	2.02	1.36	0.672
Composite 2	0.04	0.81	0.52	0.637
	0.4	2.14	1.19	0.555
Optimal composite 1	0.04	0.83	0.48	0.583
	0.4	2.11	1.26	0.600
Optimal composite 2	0.04	0.83	0.49	0.596
	0.4	2.12	1.25	0.588

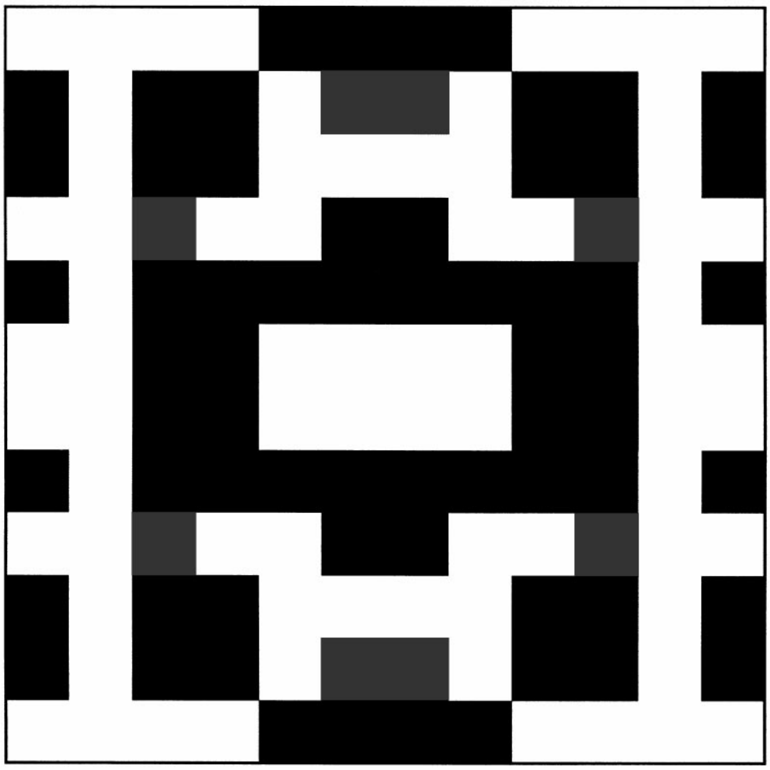

Fig. 6. Microstructure for Example 3.

$E(t) = 0.5 + 3e^{-t/10}, \quad \nu = 0.35 \quad$ for phase 1 material
$E(t) = 0.5 + 3e^{-t}, \quad \nu = 0.35 \quad$ for phase 2 material.

We are to design a microstructure of a composite which is composed of the two materials with 50% volume fraction for each material. The composite is to be used in vibrating structures with the operating frequencies, 0.04 and 0.4. By the same way as in Example 1, two composites are defined and termed as composite 1 and composite 2. The effective complex moduli of the two given materials and the two composites are listed in Table 3. The two composites show different damping characteristics at each operating frequency. At the first operating frequency, $\omega = 0.04$, the composite 2 has larger damping than the composite 1. In contrast, the composite 1 has larger damping than the composite 2 at the second operating frequency, $\omega = 0.4$. However, the differences in stiffness are not as large as the differences in damping since the two constituent materials have different relaxation times while their stiffnesses are comparable. Therefore, the design focus will be placed on the damping characteristics.

The second design example is defined as a problem to find a microstructure that yields as large damping as possible in the sense that the average value of the loss tangents at the two frequencies becomes maximum. The description of the problem is as follows.

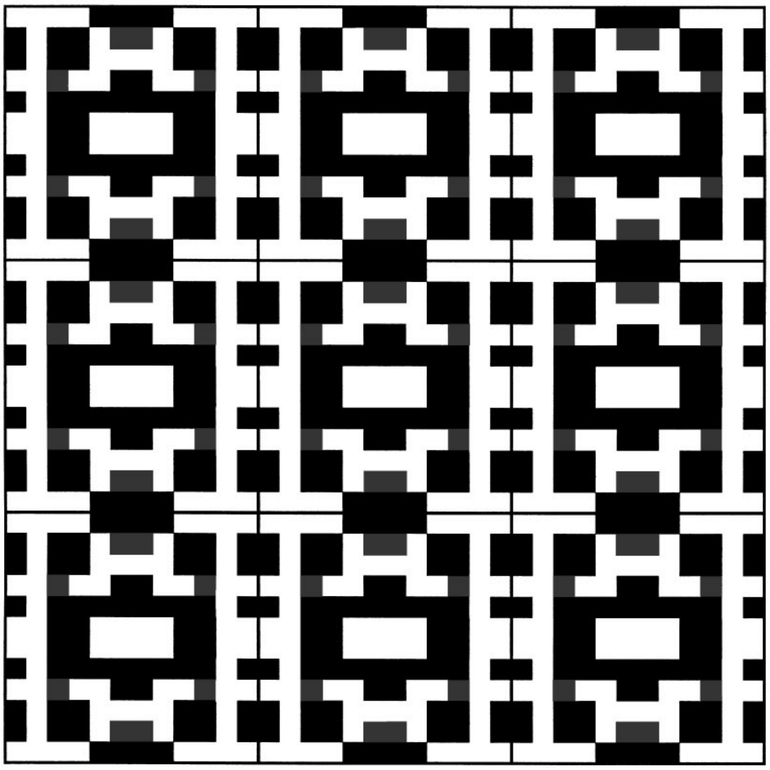

Fig. 7. Periodic microstructure for Example 3.

$$\begin{array}{ll} \text{maximize} & \tan\delta_{11}(\omega_1)+\tan\delta_{11}(\omega_2), \quad \text{where } \omega_1=0.04, \omega_2=0.4 \\ \text{subject to} & G'_{11}(\omega_1)=G'_{22}(\omega_1), \quad G'_{11}(\omega_2)=G'_{22}(\omega_2) \\ & G''_{11}(\omega_1)=G''_{22}(\omega_1), \quad G''_{11}(\omega_2)=G''_{22}(\omega_2) \\ & 50\% \text{ volume fraction for each material} \\ & \text{geometric symmetry about } X_1\text{-axis and } X_2\text{-axis.} \end{array}$$

Also, the penalty term has been added to suppress the intermediate phase of the artificial two-phase material model. Fig. 6 shows the unit cell of the optimal microstructure, for which the solution converged after 32 function calls. Fig. 7 shows the same microstructure in a 3×3 cell. The newly designed microstructure has the mechanism-like structure as in Example 1. The effective complex moduli are listed in Table 3, where optimal composite 2 is one obtained with a different initial guess although its microstructure is not presented here. The results show that a tradeoff has been made between the composite 1 and the composite 2. The difference in the loss tangent at each operating frequency is decreased compared to the composite 1 and composite 2. The loss tangent itself is greater than the smaller of those of the composite 1 and the composite 2. Fig. 8 shows the loss tangents of the two given constituent materials, the two conventional composites, and the newly designed composites as a function of frequency. It shows the improvements in damping characteristics in the range of interest. Although only two frequencies are taken as the operating frequencies of interest in this numerical experiment, the same procedure can be applied for more operating frequencies.

As in the previous elastic–viscoelastic composite design example, the present example also has the

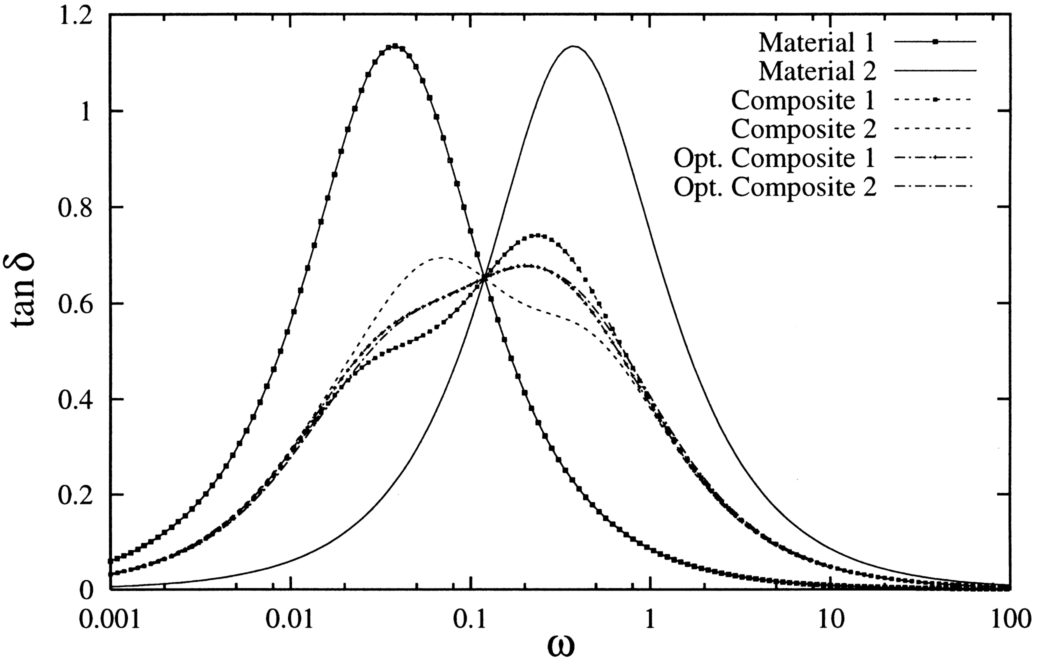

Fig. 8. Comparison of loss tangents in Example 3.

problem of numerous local minima. However, the damping characteristics of the optimal microstructures computed from different initial guesses are almost the same as shown in Fig. 8.

5. Conclusions

Optimal design of microstructures of viscoelastic composites is presented, aiming at improving stiffness and damping characteristics following the inverse homogenization approach. An inverse homogenization problem is presented as a topology optimization problem of two-phase composites. An artificial two-phase material model is introduced to simplify the problem. The sensitivities of the effective complex moduli with respect to density has a simple form: no adjoint problem has to be solved. The objective function is defined as a combination of effective complex moduli to cover up wide range of applications related to stiffness and damping characteristics. A penalty term is added to the objective function to suppress the intermediate density. Several kinds of design constraints are used to aid trade-offs between stiffness and damping characteristics and to include geometric and material symmetry conditions.

The numerical examples show that the improvements in the damping characteristics of viscoelastic composites can be achieved by designing topological structures of the composites. From the designed microstructures, it is found that mechanism-like structures and wavy structures have a crucial role in improving damping by providing sufficient deformation in viscoelastic phase while maintaining stiffness at desired level.

As with other inverse homogenization problems for elastic, thermoelastic, and piezoelectric composites, the present problem also has such numerical difficulties as mesh dependency and numerous local minima. More critical problem resides in manufacturing of the designed microstructures. Advanced manufacturing technology should be developed so that the designs are realized within a reasonable cost. Newly developed technologies such as micromachining and fabrication of molecular composites by micro-network may be possible candidates. For example, works on fabricating molecular composites at the molecular level is in progress now (Sperling, 1992).

References

Allaire, G., Kohn, R.V., 1993. Topology optimization and optimal shape design using homogenization. In: Bandsoe, M.P., Mota Soares, C.A. (Eds.), Topology Design of Structures. Kluwer Academic Publishers, Dordrecht, pp. 207–218.

Allaire, G., Bonnetier, E., Francfort, G., Jouve, F., 1997. Shape optimization by the homogenization method. Nemerische Mathematik 76, 27–68.

Arora, J.S., 1989. Introduction to Optimum Design. McGraw-Hill, New York.

Bakhvalov, N., Panasenko, G., 1989. Homogenization: Averaging Processes in Periodic Media: Mathematical Problems in the Mechanics of Composite Materials, Mathematics and Its Applications (Soviet Series). Kluwer Academic Publishers, Dordrecht.

Bendsøe, M.P., Kikuchi, N., 1988. Generating optimal topologies in structural design using a homogenization method. Computer Methods in Applied Mechanics and Engineering 71, 197–224.

Bendsøe, M.P., 1989. Optimal shape design as a material distribution problem. Structural Optimization 1, 193–202.

Bendsøe, M.P., Diaz, A., Kikuchi, N., 1993. Topology and generalized layout optimization of elastic structures. In: Bandsoe, M.P., Mota Soares, C.A. (Eds.), Topology Design of Structures. Kluwer Academic Publishers, Dordrecht, pp. 159–205.

Bendsøe, M.P., Ben-Tal, A., Zowe, J., 1994. Optimization methods for truss geometry and topology design. Structural Optimization 7, 141–159.

Bendsøe, M.P., 1995. Optimization of Structural Topology, Shape, and Material. Springer–Verlag, Berlin.

Bensoussan, A., Lions, J.-L., Papanicolaou, G., 1978. Asymptotic Analysis for Periodic Structures, Studies in Mathematics and Its Applications, vol. 5. North-Holland, Amsterdam.

Christensen, R.M., 1982. Theory of Viscoelasticity: An Introduction, 2nd ed. Academic Press, New York.

Guedes, J.M., Kikuchi, N., 1990. Preprocessing and post processing for materials based on the homogenization method with adaptive finite element methods. Computer Methods in Applied Mechanics and Engineering 83, 143–198.

Jikov, V.V., Kozlov, S.M., Oleinik, O.A., 1994. Homogenization of Differential Operators and Integral Functionals. Springer–Verlag, Berlin.

Kohn, R.V., Strang, G., 1986. Optimal design and relaxation of variational problems. Communications on Pure and Applied Mathematics 39, 113–137 (Part I), 139–192 (Part II), 353–377 (Part III).

Nelli Silva, E.C., Fonseca, J.S.O., Kikuchi, N., 1997. Optimal design of piezoelectric microstructures. Computational Mechanics 19, 397–410.

Nguyen, H.V., Pastor, J., Muller, D., 1995. A method for predicting linear viscoelastic mechanical behavior of composites, a comparison with other methods and experimental validation. European Journal of Mechanics, A/Solids 14, 939–960.

Oleinik, O.A., Shamaev, A.S., Yosifian, G.A., 1992. Mathematical Problems in Elasticity and Homogenization, Studies in Mathematics and Its Applications, vol. 26. North-Holland, Amsterdam.

Rozvany, G.I.N., Bendsøe, M.P., Kirsch, U., 1995. Layout optimization of structures. Applied Mechanics Review 48 (2), 41–119.

Sanchez-Palencia, E., 1980. Non-Homogeneous Media and Vibration Theory, Lecture Notes in Physics, vol. 127. Springer–Verlag, Berlin.

Sigmund, O., 1994. Materials with prescribed constitutive parameters: an inverse homogenization problem. International Journal of Solids and Structures 31, 2313–2329.

Sigmund, O., 1995. Tailoring materials with prescribed elastic properties. Mechanics of Materials 20, 351–368.

Sigmund, O., Torquato, S., 1997. Design of materials with extreme thermal expansion using a three-phase topology optimization method. Journal of Mechanics and Physics of Solids 45, 1037–1067.

Sperling, L.H., 1992. Introduction to Physical Polymer Science. Wiley, New York.

VMA Engineering, 1993. Dot Users Manual, Version 4.00. Vanderplaats, Miura and Associates, CA.

Yang, R.J., Chuang, C.H., 1994. Optimal topology design using linear programming. Computers and Structures 52 (2), 265–275.

Yi, Y.-M., Park, S.-H., Youn, S.-K., 1998. Asymptotic homogenization of viscoelastic composites with periodic microstructures. International Journal of Solids and Structures 35, 2039–2055.

Youn, S.-K., Park, S.-H., 1997. A study on the shape extraction process in the structural topology optimization using homogenized material. Computers and Structures 62 (3), 527–538.